Enhanced Branched-Chain Amino Acid Metabolism Improves Age-related Reproductive Function

Chen Lesnik[1,2], Salman Sohrabi[2,3], Jasmine M. Ashraf[1,2], Rachel Kaletsky[1,2], Vanessa Cota[1,2], Titas Sengupta[1,2], William Keyes[1,2], Coleen T. Murphy[1,2]*

[1]Department of Molecular Biology & [2]LSI Genomics, Princeton University, Princeton NJ 08544
[3]Department of Bioengineering, University of Texas at Arlington, Arlington, TX 76019

*Corresponding Author: ctmurphy@princeton.edu

Highlights

- BCAT-1 is abundant in mitochondria isolated from young wild-type worms and the long-lived mutant *daf-2.*
- Downregulating *bcat-1* in *daf-2* mutants reduces *daf-2* reproductive span, alters mitochondrial oocyte distribution, and elevates mtROS in mature oocytes.
- Overexpression of *bcat-1* extends reproductive capability.
- Supplementation with thiamine (vitamin B1) extends reproductive capability.

Summary

Reproductive aging is one of the earliest aging phenotypes, and mitochondrial dysfunction has been linked to a decline in oocyte quality. However, the mitochondria-related processes that are critical for oocyte quality maintenance with age have not been fully identified. We isolated mitochondria from young and aged wild-type and long-reproductive *daf-2* mutant *C. elegans* for proteomic analysis. We found that the mitochondrial proteomic profiles of young wild-type and *daf-2* worms are similar and are distinct from mitochondrial proteins of aged wild-type animals. The first enzyme of the branched-chain amino acid (BCAA) metabolism pathway, BCAT-1, is more abundant in young and *daf-2* mitochondria. Upon knockdown of *bcat-1* in *daf-2*, reproduction is shortened, mitochondrial ROS levels are elevated, and mitochondria shift to a perinuclear distribution within the mature oocytes. Moreover, *bcat-1* knockdown decreases *daf-2* oocyte quality and reduces reproductive capability in late age, indicating the importance of this pathway in the maintenance of oocyte quality with age. Importantly, we can extend reproduction in wild-type animals both by *bcat-1* overexpression and by supplementing vitamin B1, a cofactor needed for the BCAA metabolism.

Introduction

The progressive inability to reproduce increases with age in women, typically starting in the mid-30s, due to the decline of oocyte quality that precedes the onset of menopause by about 15 years[1,2]. As the maternal age for first childbirth has risen in recent years[3], understanding the mechanisms that regulate reproductive aging has become increasingly important. Compared to other tissues, oocytes visibly age early in life[4,1–3,5,65], and the decline in oocyte quality contributes to reduced reproduction with age[5,6–86,7,8,9]. The ability to reproduce late in life is determined by oocyte quality, but the factors that regulate this quality decline with age, and whether oocytes can be rejuvenated in older animals remain unclear. As in humans, the model organism *C. elegans* undergoes reproductive aging that is regulated by highly conserved genes and pathways that regulate oocyte quality with age [10]. Several *C. elegans* mutants have an extended reproductive span, including the *daf-2* insulin/IGF-1 receptor mutant[11,12]; *daf-2*'s longer reproductive span results from its ability to maintain high-quality oocytes with age[10]. The similarities in reproductive decline between humans and *C. elegans* make worms an excellent model for studying pathways that influence reproductive aging

and identifying new mechanisms that may improve reproductive longevity[13].

Mitochondria are highly abundant in oocytes, and accumulating evidence suggests a pivotal role for mitochondria in oocyte aging[14,15,16]. As human oocytes age, mitochondria activity and number decline, resulting in decreased oocyte quality[5,17,18]. However, it is not fully understood whether mitochondria dysfunction directly contributes to oocyte and reproductive aging or if it merely correlates with the observed age-related decline. Furthermore, whether therapeutics aimed at altering aged mitochondrial properties could be used to treat oocyte quality decline is unknown.

Here, using the genetic tractability of *C. elegans*, we addressed these questions by proteomically profiling and testing the role of mitochondria in wild-type and *daf-2* mutant animals with age in the context of oocyte quality and reproductive decline. To do so, we profiled the mitochondrial proteome of aged wild-type animals and *daf-2* mutants to identify "youthful" mitochondria-related proteins and then tested their involvement in reproductive aging. We found that the branched-chain amino acid (BCAA) degradation pathway regulates reproductive aging. Specifically, the first enzyme of the pathway, BCAT-1, is important for maintaining normal characteristics of mitochondria in *daf-2* oocytes. While BCAT-1 is required for *daf-2*'s extended reproductive span and normal wild-type reproductive span, loss of *bcat-1* does not affect lifespan. Modulating this pathway in wild-type worms improves oocyte quality and extends reproduction: both overexpression of *bcat-1* and supplementation with vitamin B1/thiamine, a cofactor needed for the BCAA pathway, extend late-mated reproduction. Taken together, our data link mitochondrial BCAA metabolism with aged oocyte quality and suggest that modulation of this pathway via vitamin B1/thiamine may be an effective strategy to promote reproductive longevity.

Results

Aged *daf-2* worms maintain a 'youthful' mitochondrial proteomic profile

The insulin/IGF-1 signaling (IIS) receptor mutant *daf-2* has both an extended lifespan[19] and reproductive span[12,18] (Fig. 1A). To identify a set of "youthful" mitochondria-associated proteins, we isolated mitochondria using biochemical fractionation and sequential centrifugation from young (Day 1 adult) and reproductively aged (Day 5 adult) wild-type worms and from *daf-2(e1370)* mutants (Fig. S1). Day 5 of adulthood was selected as the reproductively aged timepoint since it marks the start of oocyte quality decline in wild-type worms, while both reproduction and high oocyte quality are maintained in *daf-2* animals (Fig. 1A). Our LC-MS/MS proteomic analysis identified and quantified 1469 proteins, with a minimum of two peptides per protein and replication across a minimum of two out of three replicates (Table S1). Principal component analysis suggests that mitochondrial proteins from young wild-type and both young and aged *daf-2* worms are most similar, while aged wild-type mitochondrial proteins are most different (Fig. 1B). That is, the differences between young vs. aged *daf*-2 mitochondria are smaller than those of young vs. aged wild-type, suggesting that *daf*-2's mitochondrial proteomes undergo fewer changes within these days of adulthood than wild-type.

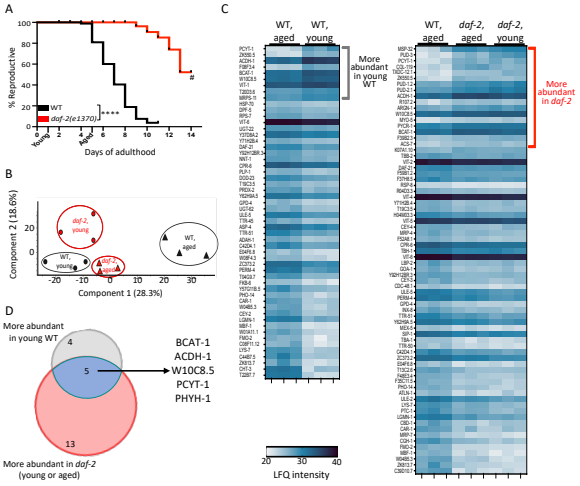

Figure 1: The mitochondrial proteome of *daf-2* is similar to young wild-type and distinct from aged wild-type

(A) *daf-2* mutants have an extended mated reproductive span. The time points of young (Day 1) and aged (Day 5) mitochondria isolation are indicated. # indicates a high matricide frequency. (B) Principal component analysis of mitochondrial proteins suggests a similarity between young wild type and young and aged *daf-2*, and distinct clustering from the aged wild-type mitochondria proteome. (C) Heat maps of the LFQ intensity of proteins that are significantly (q-val< 0.05, -1<$\log_2$ratio<1) different in *daf-2* (young & aged), or young wild type, compared to aged wild-type mitochondria (left or right, respectively). (D) Venn diagram of proteins that were more abundant in mitochondria isolated from *daf-2* and young wild-type worms compared to aged wild-type worms (5 proteins, hypergeometric p< 0.005). The intersection shows the list of shared proteins.

Proteins that are significantly more abundant in this cluster (*daf-2*, both young and aged, and young wild-type mitochondria), compared to aged wild-type mitochondria, may be indicators of mitochondria

function in the metabolic pathways important for maintaining young cellular properties and/or inhibiting age-related processes. The more abundant proteins in mitochondria isolated from *daf-2* and young wild-type worms compared to aged wild-type worms (hypergeometric *p-val*< 0.005, based on majority protein IDs, Fig. 1C, D) include BCAT-1 (branched chain aminotransferase), ACDH-1 (acyl CoA deyydrogenase/*dod-12*), W10C8.5, PCYT-1 (phosphocholine cytidylyltransferase), and PHYH-1 (phytanoyl-CoA hydroxylase). Notably, two of these proteins are enzymes in the branched-chain amino acid (BCAA) degradation pathway: BCAT-1 is an ortholog of human BCAT1 and BCAT2, and ACDH-1 is an ortholog of human ACADSB, suggesting that this pathway could be important for maintaining mitochondrial function with age in both wild-type and *daf-2* worms. ACDH-1 is also involved in lipid metabolism, as is as PHYH-1, which is predicted to be involved in fatty acid alpha-oxidation. W10C8.5 is an ortholog of several human genes, including creatine kinase B and creatine kinase mitochondrial 1B, while PCYT-1 catalyzes the transfer of phosphocholine in the phosphatidylcholine biosynthetic process.

bcat-1 is important for *daf-2*'s lifespan, extended reproduction, and high-quality oocytes with age

To determine whether the BCAA degradation pathway is important for *daf-2*'s youthful characteristics, we focused on the first enzyme of the pathway, *bcat-1*. We first tested whether *bcat-1* is required for *daf-2*'s extended longevity. Adult-only RNA interference (to avoid any defects caused by *bcat-1* loss in development) of *bcat-1* significantly shortens *daf-2*'s lifespan (16.62%, *p*- value<0.0001, Fig. 2A, Table S3).

The *C. elegans* germline is the main tissue where mtDNA replicates, and the germline contains the majority of mtDNA in the adult worm[20], consistent with the energy-intensive role of the germline in reproduction[20–22]. We previously found that *acdh-1* is required for *daf-2's* extended lifespan[23]. To determine whether *bcat-1* is also important for maintaining *daf-2*'s reproduction with age, we used adult-only RNAi treatment to determine the late-mated reproduction of aged *daf-2* worms. Indeed, reduction of *bcat-1* significantly reduced *daf-2*'s reproductive ability with age (Fig. 2, C, Table S4).

Previously, we found that *daf-2's* ability to reproduce late in life is due to its improved oocyte quality maintenance with age[10]. While oocyte quality decline is observed in wild-type worms as early as Day 5, *daf-2* animals maintain high-quality oocytes late into the reproductive period, which promotes its extended reproduction. Since *bcat-1* is required for *daf-2's* extended reproductive span, we next asked whether *bcat-1* knockdown impairs *daf-2*'s ability to maintain oocyte health. On Day 7 of adulthood, mated *daf-2* animals on control RNAi maintain uniformly sized, cuboidal-shaped oocytes, aligned one next to each other in the proximal end of the gonad[10] (Fig. 2D, control). However, *daf-2* mutants treated with *bcat-1* RNAi display misshapen and small oocytes and significant germline abnormalities (Fig. 2D, E). These results demonstrate that BCAT-1 is required for *daf-2*'s ability to extend reproductive span by maintaining high-quality oocytes with age.

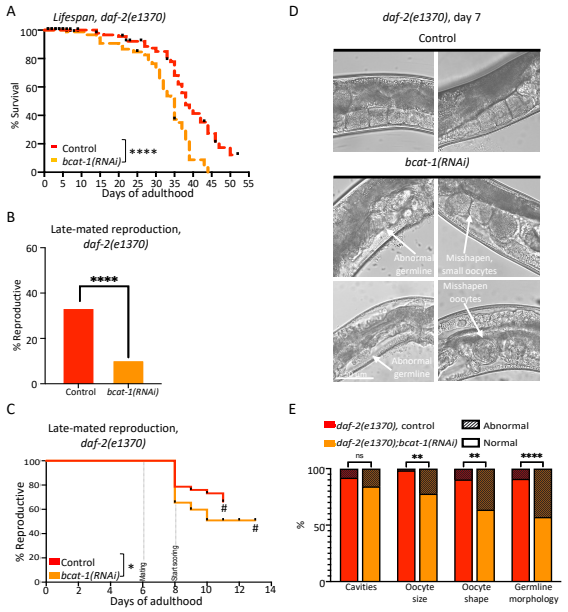

Figure 2: Downregulating *bcat-1* in *daf-2* reduces lifespan, reproductive capability, and oocyte quality

(A) Adult-only knockdown of *bcat-1* shortens the lifespan of *daf-2.* Representative graph (see Fig. S2, Table S3 for replicates). Lifespan data are plotted as Kaplan-Meier survival curves, and the *p*-value was calculated using Mantel-Cox log-ranking (****$p \leq 0.0001$, ns= not significant). n= 120 for each condition. (B+C) RNA interference reduction of *bcat-1* decreases the late-mated reproduction of adult *daf-2* at Day 8 as scored either (B) every day after mating (n= 75 for control, n= 58 for *bcat-1(RNAi)*, *$p \leq 0.05$), or (C) 5 days after mating (more than 3 biological replicates were performed representative graph n= 104 for control, n= 103 for *bcat-1(RNAi).* Chi-square tests, ****$p \leq 0.0001$). (D) *bcat-1* is required for oocyte and germline quality maintenance in *daf-2* animals (representative images), as scored (E) based on oocyte quality criteria. Representative graph is shown. 3 biological replicates were performed. n= 67 for control, n= 57 for *bcat-1(RNAi).* Chi-square tests. ns = not significant, **$p \leq 0.01$, ****$p \leq 0.0001$.,

bcat-1 reduction alters mitochondria localization, mtROS production, and mitochondria activity

Since *bcat-1* is required for *daf-2*'s maintenance of oocyte quality and slowed reproductive aging, and BCAT-1 is a mitochondrial protein[24] (Fig. 1), we next examined how *bcat-1* knockdown affects germline mitochondria morphology. To visualize germline mitochondria, we used a *daf*-2 strain expressing the outer mitochondrial membrane protein TOMM-20 fused to mKate2 specifically in the germline. Under control RNAi conditions, mitochondria are uniformly distributed in the mature oocytes (Fig. 3A). However, adult-only knockdown of *bcat-1* induces clustering of mitochondria in a perinuclear localization in *daf-2* mature oocytes (Fig. 3A, B, inset, Supp. Videos 1-3).

Perinuclear mitochondria distribution has been previously associated with cellular stress and changes in cellular ROS levels[25]. Therefore, we wanted to test whether BCAA metabolism affects mtROS in aged *daf*-2 oocytes. Unlike wild-type oocytes, which show increased mtROS levels with age, *daf-2* maintains low mtROS in the most mature oocyte (the -1 oocyte) with age (Fig. 3C, D). However, mtROS levels are higher in Day 5 *daf-2;bcat-1(RNAi)* oocytes compared to the control (Fig. 3E, F), suggesting that *bcat-1* is essential for maintaining low levels of cellular mitochondrial ROS.

High mitochondrial ROS may be caused by increased mitochondrial activity. To specifically assess mitochondria activity in mature oocytes, we used tetramethylrhodamine ethyl ester (TMRE), a dye that labels active mitochondria through increased mitochondrial membrane potential. We found that *bcat-1* knockdown increased TMRE fluorescence intensity in *daf-2* oocytes, indicating mitochondrial hyperactivity (Fig. 3G, H).

Together, these results indicate that altered BCAA metabolism via *bcat-1* knockdown disrupts mitochondrial cellular distribution and promotes hyperactive mitochondria in *daf-2* oocytes. This knockdown is also associated with elevated mtROS levels in aged oocytes, like those observed in wild-type oocytes with age. These changes upon reduction of BCAT-1 may contribute to the accelerated decline of *daf-2* oocyte quality and reduction of reproductive span.

bcat-1 overexpression extends reproduction and improves oocyte quality in wild-type animals

BCAT-1 was among the 'youthful' mitochondrial

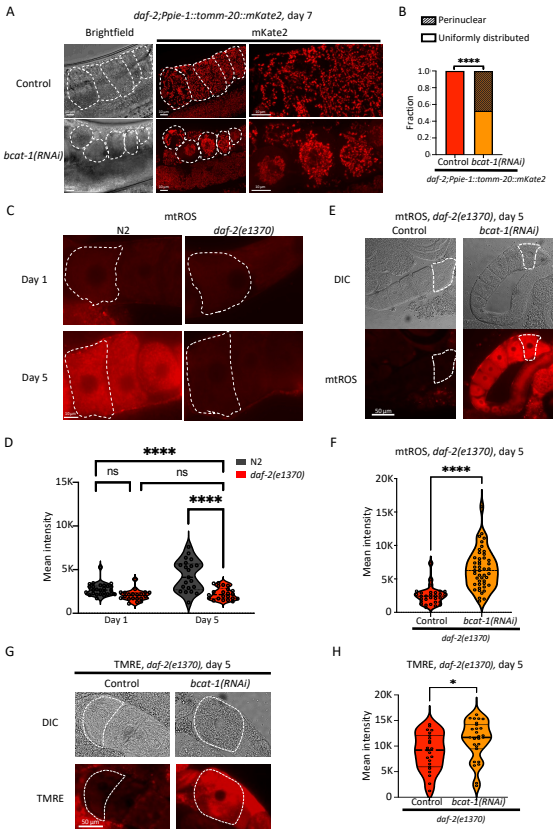

Figure 3: *bcat-1* knockdown in *daf-2* mutants alters mitochondria cellular localization, mtROS levels, and mitochondria activity
(A) Adult-only *bcat-1* knockdown results in the perinuclear localization of mitochondria in *daf-2::Ppie-1::tomm-20::mKate2* oocytes on day 7. A white dashed outline marks mature oocytes. (B) Quantification of perinuclear mitochondria in localization of mitochondria in *daf-2::Ppie-1::tomm-20::mKate2* oocytes on day 7. Representative graph from 3 biological replicates. n= 36 for control, n= 44 for *bcat-1(RNAi).* Chi-square test. ***$p \leq 0.0001$. (C) mtROS levels are increased on day 5 in the mature oocyte of wild-type animals, but not *daf-2,* (compared to day 1). A white dashed outline marks the most mature oocyte (-1 oocyte). (D) Quantification of mtROS (mean intensity) in -1 oocyte in wild-type animals compared to *daf-2*, day 1 vs. day5 of adulthood. n>20 for all conditions, Two-way ANOVA. ns = not significant, ****$p \leq 0.0001$. (E) mtROS levels are increased in *daf-2* mature oocytes on Day 5 upon adult-only *bcat-1* knockdown. A white dashed outline marks the most mature oocytes (-1 oocytes). (F) mtROS levels in *daf*-2 mature oocytes on day 5 upon adult-only *bcat-1* knockdown. n= 30 for control, n= 46 for *bcat-1 (RNAi).* Two-tailed, unpaired t-test. ****$p \leq 0.0001$. (G) Mitochondria activity is higher in *daf*-2 mature oocytes on day 5 upon adult-only *bcat-1* knockdown. A white dashed outline marks the most mature oocytes (-1 oocytes). (H) Quantification of TMRE signal in *daf-2* mature oocytes on Day 5 upon adult-only *bcat-1* knockdown. n>20 for all conditions. Two-tailed, unpaired t-test. *$p \leq 0.05$. For all panels, representative images and graphs from 3 biological replicates are shown.

proteins detected in *daf-2* and young wild-type worms; therefore, we next asked whether loss of *bcat-1* affects wild-type reproduction, and conversely, whether manipulation of BCAA metab-

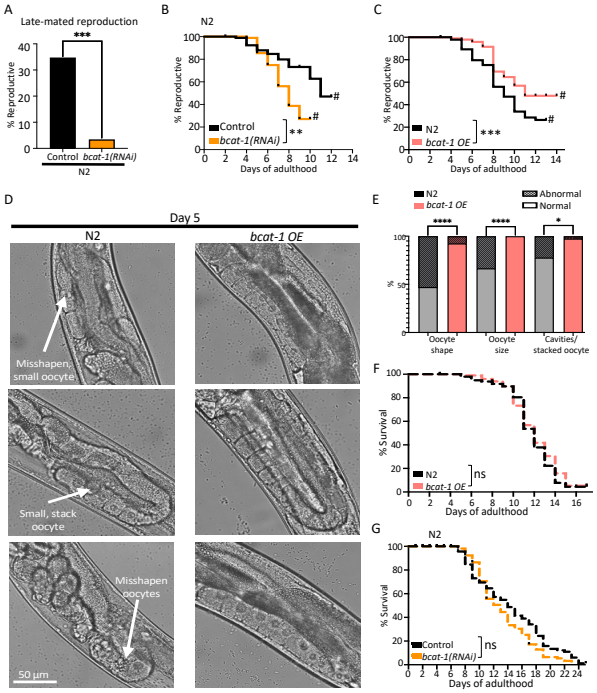

Figure 4: Knocking down *bcat-1* reduces the reproductive capability of wild-type worms, while its overexpression improves wild-type oocyte quality and extends reproductive span

(A) Downregulation of *bcat-1* reduces the late-mated reproduction of adult wild type at day 6. n= 69 for control, n= 58 for *bcat-1(RNAi).* Chi-square test. ****$p \leq 0.0001$. (B) Knocking down *bcat-1* shortens the mated reproductive span of wild-type worms. n= 100 for control, n= 90 for *bcat-1(RNAi).* **$p \leq 0.01$. (C) Overexpressing *bcat-1* extends mated reproductive span (n= 100 for wild type, n= 90 for *bcat-1* OE, ***$p \leq 0.005$. (D, E) A strain overexpressing *bcat-1* (*bcat-1* OE) maintains better oocyte quality with age. n= 36 for wild-type, n= 40 for *bcat-1* OE. ****$p \leq 0.0001$, *$p \leq 0.05$. (F,G) *bcat-1* knockdown and overexpression do not affect the lifespan of wild-type animals. n= 120 for each of the control and *bcat-1(RNAi).* # indicates a high matricide frequency. Reproductive span and lifespan data are plotted as Kaplan-Meier survival curves, and the *p*-value was calculated using Mantel-Cox log ranking (ns= not significant). For all panels, representative images and graphs from 3 biological replicates are shown.

olism via increased BCAT-1 could improve reproductive maintenance with age. Since *bcat-1* is required for *daf-2*'s extended reproductive span, we first tested whether loss of *bcat-1* would similarly impair reproduction in wild-type worms. Both the late mated reproduction (Fig. 4A) and the reproductive span (Fig. 4B, Table S2) of wild-type worms are reduced upon *bcat-1* knockdown, demonstrating that *bcat-1* is required for normal reproduction.

We next asked whether increasing BCAT-1 levels could slow reproductive decline; indeed, overexpression of *bcat-1* significantly extends reproductive span (Fig. 4C, Table S2). To determine whether *bcat-1* overexpression similarly improves oocyte quality with age, we examined oocytes on Day 5 of adulthood following mating; *bcat-1* overexpression significantly improved oocyte quality relative to wild-type controls (Fig. 4D, E). These results suggest that increased levels of BCAT-1 are sufficient to improve reproductive aging and oocyte quality in wild-type *C. elegans*.

We also tested the role of *bcat-1* levels in lifespan (Fig. 4F, G, Table S3); although it was previously suggested that *bcat-1* knockdown extends lifespan and that *bcat-1* overexpression reduces lifespan[26], we found that neither knockdown or overexpression of *bcat-1* affected lifespan (Fig. 4F, G, Fig. S2, Fig. S3, Table S3). Thus, *bcat-1* levels appear to specifically regulate oocyte quality and reproductive aging but have no role in the regulation of lifespan in wild-type animals.

Supplementation with vitamin B1 slows reproductive decline in wild-type worms

BCAT-1 catalyzes the first step of the catabolism of the branched-chain amino acids (BCAAs) (Fig. 5A). To test whether knockdown of *bcat-1* would directly result in higher BCAA levels in aged *daf-2* animals, we knocked down *bcat-1* and assessed BCAA levels using a quantitative colorimetric assay[27]. Indeed, BCAA levels are increased in aged *daf-2* worms upon adult-only *bcat-1* knockdown, indicating that reduction of *bcat-1* is sufficient to alter BCAA metabolism (Fig. 5B). Our findings suggest that maintaining BCAT-1 levels with age extends reproduction by maintaining flux through the BCAA pathway.

Since BCAT-1 functions in the BCAA metabolic pathway (Fig. 5A), we hypothesized that other treatments that affect BCAA metabolism downstream of BCAT-1 might similarly improve reproductive aging in *C. elegans*. The rate-limiting reaction of the BCAA metabolism pathway is catalyzed by the branched-chain α-keto acid dehydrogenase (BCKDH) complex[28,29] (Fig. 5A). This mitochondrial enzymatic complex functions downstream of BCAT-1, converting the α-keto acids of each branched-chain amino acid to the corresponding acyl CoAs. BCKDH is composed of three subunits, E1, E2, and E3. The E1 subunit binds thiamine pyrophosphate (ThPP), which is an essential cofactor and a derivate of thiamine, also known as vitamin B1[30]. Animals cannot synthesize thiamine and rely on its absorption from their diet. After being imported into animal cells, thiamine is transformed into ThPP by thiamine pyrophosphokinase[31,32]. When thiamine levels are insufficient, BCAA catabolism is

impaired, increasing the levels of unprocessed branched-chain keto acids[33]. To test whether supplementation of vitamin B1 would extend reproductive aging, we supplemented vitamin B1 starting on the first day of adulthood; this treatment significantly extends the mated reproductive span of wild-type worms, increasing median reproductive span by more than 30 percent (Fig. 5C, Table S2), and slightly extends lifespan (Fig. 5D, Table S3). Moreover, aged oocytes of animals supplemented with vitamin B1 were significantly higher in quality (Fig. 5E, F).

Mitochondrial ROS (mtROS) levels are elevated in both aged wild-type and aged *daf-2(e1370);bcat-1(RNAi)* worms (Fig. 3C-F). Because supplementing vitamin B1 during adulthood is sufficient to improve oocyte quality with age and to extend reproduction, we next tested whether supplemention with vitamin B1 also reduces mtROS in aged oocytes. Indeed, aged oocytes of animals supplemented with vitamin B1 have significantly lower levels of mtROS compared to untreated animals (Fig. 5G, H). Together, these data suggest that the addition of a dietary supplement starting in adulthood is sufficient to improve oocyte quality, thus extending reproductive ability with age at least in part through a reduction in mtROS levels in aged oocytes.

Discussion

Here, we identify BCAT-1 and the branched-chain amino acid pathway as a potential oocyte quality and reproductive aging regulator. The mitochondria proteomic profile of young wild-type animals is similar to that of young and old *daf-2* insulin/IGF-1 longevity mutants, while the mitochondrial proteomic profile of aged wild-type animals is distinct; the level of BCAT-1 is one of the principal differences in these profiles. Using *daf-2* as a tool to study extended reproductive span, we found that the BCAA catabolism pathway is important for the ability to maintain reproduction with age, through the maintenance of mitochondrial localization, normal mitochondrial activity, and low mtROS levels. Our results suggest that high levels of BCAT-1 are associated with high-quality oocytes and reproductive longevity. Conversely, high oocyte mtROS levels, either due to age or to the stress caused by *bcat-1* reduction, are linked to poor oocyte quality and reduced reproduction.

The BCAA pathway includes several enzymes, including the BCKD complex, which uses thiamine as a co-factor (Fig. 5A). Thiamine is the precursor for

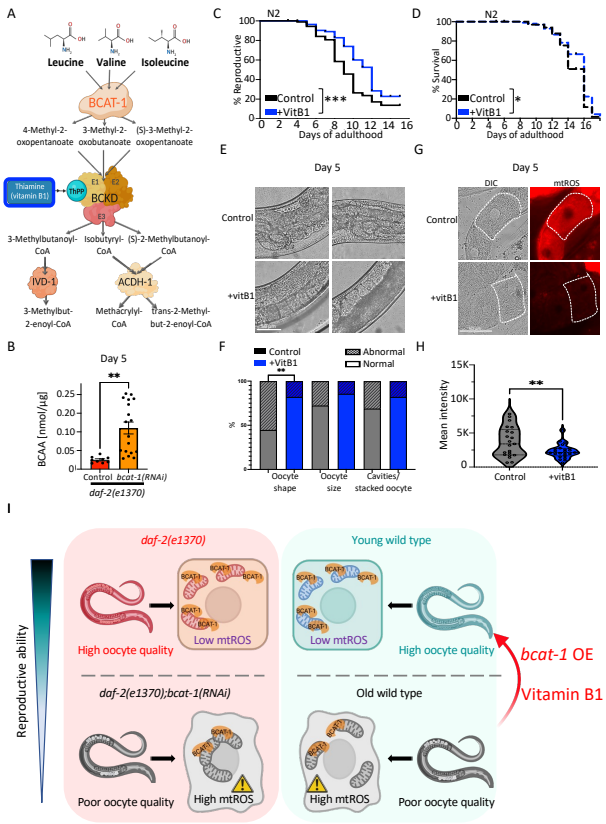

Figure 5: Adult-only supplementation of vitamin B1 improves wild-type oocyte quality and extends reproductive span

(A) Scheme of selected steps in the branched-chain amino acid metabolism pathway in *C. elegans*. (B) Quantitative colorimetric assay confirms that BCAA levels are increased in Day 5 *daf-2* worms after adult-only *bcat-1* knockdown. Each dot represents a different measurement of BCAA concentration from a lysate of at least 70 worms. All measurements from a total of 3 biological replicates are shown. Two-tailed, unpaired t-test. $^{**}p \leq 0.001$. (C) Supplementing with 5 mg/mL of thiamine (vitamin B1) starting on day 1 of adulthood significantly extends the mated reproductive span of wild-type animals. n= 90 for control, n= 88 for +vitamin B1 condition (representative graph of 3 biological repeats. # indicates a high matricide frequency. $^{***}p \leq 0.0005$), and slightly extends lifespan (3%, $p<0.05$) (D). (E,F) Adult-only supplementation of vitamin B1 is sufficient to maintain better oocyte quality with age (E). (F) Graph of Day 5 oocytes as scored based on quality criteria. n> 25 for each condition. Chi-square test. $^{**}p \leq 0.005$, ns = not significant. (G, H) mtROS levels were significantly lower in the Day 5 mature oocytes of wild-type worms supplemented with vitamin B1. A white dashed outline marks the most mature oocyte (-1 oocytes). Representative images. (H) Representative graph of 2 biological repeats. n> 20 for each condition. Two-tailed, unpaired t-test. $^{**}p \leq 0.005$ (I) Model: *bcat-1* is important for mitochondria organization and mtROS levels in *daf-2* mature oocytes. Upon its downregulation, mitochondria are altered, and oocyte quality is poor, resulting in a shorter reproductive span (top). *bcat-1* is important for wild-type reproduction. We hypothesized that its levels are reduced with age, resulting in reduced reproduction. By overexpressing *bcat-1* or by supplementing with vitamin B1 during adulthood, reproduction can be extended (bottom).

several phosphorylated derivatives, and its pyro-phosphate form is an essential co-factor for enzymatic complexes involved in carbohydrate and amino acid metabolism. As the human body cannot synthesize thiamine, its levels depend on dietary intake[34–36]. Thiamine-deficient diets can cause a disease known as "Beriberi" which affects the normal function of various systems in the human body, including the cardiovascular and nervous systems[35].

Thiamine deficiency is considered rare in the US and elsewhere due to the low daily recommended requirements (defined in the US in the 1940s) and the introduction of thiamine-fortified foods, leading to increased dietary intake. The perception that most individuals receive enough thiamine has led to reduced routine testing for thiamine deficiency, such that the NIH states that there are "no current data on the rates of thiamine deficiency in the U.S. population" [36]. However, recent findings suggest that thiamine deficiency may be underappreciated, with 10-90% of subjects across several studies, including studies of obesity, diabetes, pregnancy, psychiatric illness, neurodegenerative disease, aging, and hospitalized patients, exhibiting various aspects of thiamine deficiency[33]. This is despite many individuals regularly consuming more than the recommended daily intake[33]. Since thiamine absorption and bioavailability are impacted by age, diet composition, genetic and epigenetic factors, medication use, and illness, Marrs & Lonsdale, 2021 suggest that thiamine is required beyond the current recommendations for the greater population[33]. No adverse effects have been reported for thiamine supplementation[37], suggesting that this is a safe intervention to increase available thiamine levels, and as our study suggests, potentially may increase oocyte quality in females with age.

As mitochondrial pathways are highly conserved, and pathways that are misregulated with age in women's oocytes are similar to those that change with age in *C. elegans*[17], dietary supplementation of vitamin B1, which is generally reported as safe to use as a supplement, might have similar beneficial effects on oocytes and reproduction with age in higher organisms as well. Our results suggest that *C. elegans* reproductive aging findings may be relevant for improving human oocyte health with age.

Acknowledgments

We thank Henry Shwe and Saw Kyin (Princeton Proteomics and Mass Spectrometry Core) for their assistance in sample processing and MS instrumentation, Gary Laevsky and Sha Wang (the Confocal Imaging Facility, a Nikon Center of Excellence, in the Department of Molecular Biology at Princeton University), The De Botton Protein Profiling institute of the Nancy and Stephen Grand Israel National Center for Personalized Medicine Weizmann Institute of Science (Dr. Yishai Levin), Princeton Genomics Core Facility, the Petry lab and the Gitai lab (the Department of Molecular Biology at Princeton University) for helping with equipment, the *Caenorhabditis* Genetics Center (CGC) for strains, and Murphy Lab members for comments on the manuscript. The study was supported by the Global Consortium for Reproductive Longevity and Equality to CTM (AWD1006679).

Materials and Methods

Bacteria strains

Strain	Source
E. coli: OP50	Caenorhabditis Genetics Center
E. coli: HT115	Caenorhabditis Genetics Center

***C. elegans* strains**

Strain	Source	Identifier	Ref.
N2 var. Bristol: wild type	*Caenorhabditis* Genetics Center	Wild-type worms	
daf-2(e1370) III	Shen's lab	CB1370	
fog-2(q71)		CB4108	
risIs3 [K02A4.1p::K02A4.1::GFP + unc-119(+)]	Caenorhabditis Genetics Center	MIR23	[26]
foxSi27 [Ppie-1::tomm-20::mKate2::HA::tbb-2 3' UTR (oxti385)] I	Gift from Dr. Steven Zuryn's lab	SJZ106	[39]
foxSi27 [Ppie-1::tomm-20::mKate2::HA::tbb-2 3' UTR (oxti385)] I; daf-2(e1370) III	This paper	CQ650	

Reagents

	Source	Cat #
Percoll, pH 8.5-9.5	Sigma	P1644
10X Bolt Sample Reducing Agent	Invitrogen	B0009
4X Bolt LDS Sample Buffer	Invitrogen	B0007
gradient-PAGE (4 % -12 %) Bis-Tris gel	Invitrogen	NW04125BOX
Immobilon-P PVDF Membrane	Millipore	IPVH00010
Anti-Histone H3 antibody - Nuclear Marker and ChIP Grade	abcam	ab1791
Anti-ATP5A antibody [15H4C4] - Mitochondrial Marker	abcam	ab14748
Anti-PDHA1 antibody [8D10E6]	abcam	ab110334
Anti-α-Tubulin antibody, Mouse monoclonal	Sigma	T6074
Goat Anti-Mouse IgG H&L (HRP)	abcam	ab205719
Goat Anti-Rabbit IgG H&L (HRP)	abcam	ab6721
CL-XPosure™ Film, 7 x 9.5 in. (18 x 24 cm)	Thermo Scientific	34089
Branched Chain Amino Acid Assay Kit / BCAA Assay Kit	abcam	ab83374
Quant-iT™ Protein Assay Kit	Invitrogen	Q33210
MitoTracker™ Red CM-H2Xros - Special Packaging	Invitrogen	M7513
Thiamine hydrochloride (synonym: vitamin B1 hydrochloride)	Sigma	T1270
TMRE	Invitrogen	T669

***C. elegans* genetics and maintenance**

C. elegans strains were cultured using standard methods[38]. Worms were maintained at 20°C on plates made from either nematode growth-medium (NGM): 3 g/L NaCl, 2.5 g/L Bacto-peptone, 17 g/L Bacto-agar in distilled water, with 1 mL/L cholesterol (5 mg/mL

stock in ethanol), 1 mL/L of 1 M CaCl2, 1 mL/L of 1 M MgSO4, and 25 mL/L of 1 M potassium phosphate buffer (pH 6.0) added to molten agar after autoclaving, or HGM: 20 g/L Bacto-peptone, 30 g/L Bactoagar, and 4 mL/L cholesterol, with all other components same as NGM. Plates were seeded with OP50 *E. coli* for ad libitum feeding. For synchronizing worms, gravid hermaphrodites were exposed to a 15% hypochlorite solution (8.0 mL water, 0.5 mL of 5N KOH, 1.5 mL sodium hypochlorite) to collect eggs, which were then washed in M9 buffer (6 g/L Na2HPO4, 3 g/L KH2PO4, 5 g/L NaCl and 1 mL/L of 1M MgSO4 in distilled water) before transferring to seeded plates.

For RNAi experiments, the standard NGM molten agar was supplemented with 1 mL/L of 1M IPTG (isopropyl β-d-1-thiogalactopyranoside) and 1 mL/L of 100 mg/mL carbenicillin (RNAi plates). Plates were seeded with HT115 *E. coli* containing the RNAi plasmid or empty control vector (L4440). RNAi clones were obtained from the Ahringer RNAi library and induced with 0.1 M IPTG 1 hour prior to transfer, starting at adulthood. Worms were transferred to freshly seeded plates every other day when producing progeny, unless otherwise specified. sequence verified. For all RNAi experiments, worms were transferred to RNAi plates that were pre-

Mitochondria purification for mass spectrometry and proteomic analysis

Synchronized *C. elegans* were maintained on HGM agar plates seeded with *E. coli* OP50 as the food source. Every two days, worms were washed off plates with M9 buffer and were transferred to fresh plates to avoid progeny accumulation. Mitochondria were isolated using the following optimized protocol modified from previously described methods[39–42].

Worms at the appropriate adult stage (as indicated per experiment) were washed off plates with M9 buffer and transferred to HGM agar plates that were spotted with 5 mg/mL serotonin to induce egg laying. After incubation for 2 hours at 20°C, worms were collected from plates and washed five times with M9 buffer. Worms were then washed with ice-cold 0.1 M NaCl, pelleted at 1100 x g for 5 minutes at room temperature, and resuspended with an ice-cold mix of 0.1 M NaCl and 60% sucrose (1:1 v/v ratio). Animals were centrifuged at 1100 x g for 5 minutes, and floating worms were collected and diluted 1:4 in 0.1 M NaCl. Worms were then washed twice with 0.1 M NaCl and then resuspended in mitochondria isolation buffer (MIB: 50 mM KCl, 110 mM mannitol, 70 mM sucrose, 0.1 mM EDTA, pH 8.0, 5 mM Tris-HCl, pH 7.4). The resuspended worms were then transferred to a cold glass 2 mL Dounce homogenizer (KIMBLE KONTES # 885300-0002) and were homogenized using 20 strokes (B pestle). To remove nuclei and cell debris, the homogenate was centrifuged at 750 x g for 5 min at 4 °C. The supernatant was collected and set aside at 4 °C, while the pellet was resuspended in MIB for an additional round of Dounce homogenization to maximize yields. Following centrifugation at 750 x g for 5 min at 4 °C, the supernatant was pooled with the supernatant collected in the first Dounce step. To remove any residual cell debris and bacteria, the homogenate was filtered through a 5 µm pore size hydrophilic PVDF membrane syringe filter. An aliquot of the homogenate representing cytosolic and membrane cellular fractions was kept for western blot analysis and labeled as the 'C+M' sample. The homogenate was then centrifuged at 9000 x g for 10 minutes 4 °C. An aliquot of the supernatant representing the cytosolic fraction was kept for western blot analysis, labeled as the 'C' sample, and the remaining supernatant was discarded. The resulting pellet (crude mitochondria) was washed with MIB and centrifuged at 10,000 x g for 10 minutes 4 °C. The pellet was then resuspended with ice-cold mitochondria resuspension buffer (MRB: 225 mM mannitol, 5 mM HEPES, pH 7.4, 0.5 mM EGTA), and an aliquot of the crude mitochondria was kept for western blot analysis, labeled as the 'M' sample. The crude mitochondria fraction was further purified over a Percoll gradient [43–45]; the crude mitochondria suspension was layered on top of a Percoll medium (225 mM mannitol, 25 mM HEPES, pH 7.4, 1 mM EGTA, 30% Percoll (v/v)). Samples were then centrifuged at 95,000 x g for 30 minutes using an Optima XE-100 Beckman centrifuge (SW55Ti rotor). 1 mL fractions were collected, and a sample of each was kept for western blot analysis. The pure mitochondria (Mp) were further diluted in MRB and centrifuged at 6,300 x g for 10 minutes to remove residual Percoll. The pure mitochondria pellet was washed and resuspended with MRB. All samples were frozen in liquid nitrogen and kept at -80°C until use.

Western blot analysis

For western blot analysis, samples were mixed with 10X Bolt Sample Reducing Agent and 4X Bolt LDS Sample Buffer. Samples were then heated at 70°C for 10 minutes before loading on a gradient-PAGE (4 % - 12 %) Bis-Tris gel. After their separation, samples were transferred to a PVDF membrane and blocked

with 5 % milk in TBST (10X TBST: 200 mM Tris-HCl, pH 7.5, 1.5 M NaCl, 1% Tween20). Membranes were incubated with one of the following primary antibodies: anti-Histone H3 (1:5,000 dilution), anti-ATP5A (1 μg/mL), anti-pyruvate dehydrogenase complex (1:1,000 dilution, anti-PDHA1), or monoclonal anti-αTUBULIN (2 mg/mL). After washing with TBST, membranes were incubated with the corresponding secondary antibody (either goat anti-mouse IgG H&L (HRP), 1:10,000 dilution, or goat anti-rabbit IgG H&L (HRP), 1:10,000 dilution). Membranes were then washed with TBST and imaged using CL-XPosure Film.

Mass spectrometry and proteomic analysis

Samples were dissolved in 5% SDS (Sigma #05030) and 50 mM TEAB buffer (Sigma # T7408). Trypsin digestion was performed using S-Trap micro spin columns according to the manufacturer's protocol (*S-Trap™*, PROTIFI).

Trypsin-digested samples were dried completely in a SpeedVac and resuspended with 20 µl of 0.1% formic acid, pH 3.0. Two microliters (about 360 ng) were injected per run using an Easy-nLC 1200 UPLC system. Samples were loaded directly onto a 50 cm long 75 µm inner diameter nano capillary column packed with 1.9 µm C18-AQ resin (Dr. Maisch, Germany) mated to metal emitter in-line with an Orbitrap Fusion Lumos (Thermo Scientific, USA). Easy-Spray NSI source was used. Column temperature was set at 45°C, and the two-hour gradient method with 300 nL per minute flow was used (with Buffer A: 0.1% formic acid in water, Buffer B: 0.1% formic acid in 80% acetonitrile and 20% water). The mass spectrometer was operated in data-dependent mode with a resolution of 120,000 for MS1 scan (positive mode, profile data type, AGC gain of 4e5, maximum injection time of 54 sec, and mass range of 375-1500 m/z) in Orbitrap followed by HCD fragmentation in ion trap with 35% collision energy. Charge states of 2 to 7 were included for MS/MS fragmentation. Dynamic exclusion list was invoked to exclude previously sequenced peptides for 60s and maximum cycle time of 3s was used. Peptides were isolated for fragmentation using a quadrupole (1.2 m/z isolation window). Ion-trap was operated in Rapid mode. Raw data were analyzed using the MaxQuant software suite 1.6.6.0 [47] and the Andromeda search engine. The data were queried with the Andromeda search engine against the *C. elegans,* and *E. coli* proteome databases appended with common lab protein contaminants. The higher-energy collisional dissociation (HCD) MS/MS spectra were searched against an in silico tryptic digest of *C. elegans* proteins from the UniProt/Swiss-Prot sequence database (v. 2019_09) containing 27,028 sequences, including common contaminant proteins. All MS/MS spectra were searched with the following MaxQuant parameters: acetyl (protein N-terminus), M oxidation; cysteine carbamidomethylation was set as fixed modification; max 2 missed cleavages and precursors were initially matched to 4.5 ppm tolerance and 20 ppm for fragment spectra. Peptide spectrum matches and proteins were automatically filtered to a 1% false discovery rate based on Andromeda score, peptide length, and individual peptide mass errors. Proteins were identified and quantified based on at least two unique peptides and the label-free quantification (LFQ)[48] values reported by MaxQuant. The resulting protein groups were imported into Perseus [49]. Data were filtered to include proteins identified with 2 peptides or more and those replicated in at least two of three replicates in at least one group. The data were log2 transformed, and a student's t-test was used to identify statistically significant proteins. Significant proteins were considered as proteins with more than 1 peptide per protein, fold change higher than 2, and FDR> 0.05. Enrichment analyses were performed using g:Profiler[50].

BCAA assay

Assays were performed using the Branched Chain Amino Acid Assay Kit (abcam, ab83374) according to the manufacturer's manual with the following modifications: At least 70 worms per condition were Dounce homogenized in 500 µl assay buffer. Reads were normalized to total protein concentration as measured using the Quant-iT Protein Assay Kit. OD was measured at 450 nm using the Synergy MX microplate reader.

mtROS assay

For RNAi experiments, synchronized hermaphrodites were transferred to RNAi plates at L4 stage and were transferred to fresh RNAi plates every two days to avoid progeny accumulation. For all other experiments, NGM plates were used. For assays testing vitamin B1, OP50-seeded NGM plates were used either with or without 5 mg/mL vitamin B1. One day prior to imaging, worms were transferred to seeded plates with 20 µM MitoTracker Red CM-H2Xros. On the day of imaging (either day 1 or day 5 of adulthood), worms were recovered for 1 hour on

seeded RNAi plates without MitoTracker Red CM-H2Xros. Worms were then put on slides with levamisole and were dissected for germline imaging. Images were captured on a Nikon eclipse Ti at 60x magnification, focusing on the most mature oocyte (-1 oocyte). All figures shown were from the same experiment, imaged under the same conditions. All images in each figure were processed in the same way across the entire image (e.g., adjusting for brightness and contrast).

TMRE assay

Synchronized hermaphrodites were transferred to RNAi plates at L4 stage and were transferred to fresh RNAi plates every two days to avoid progeny accumulation. A 0.5 M stock solution of Tetramethylrhodamine, Ethyl Ester, Perchlorate (TMRE, Invitrogen #T669) was prepared in DMSO and kept at -20°C. One day prior to imaging, worms were transferred to seeded RNAi plates with 1 mM TMRE (diluted in M9 buffer). On the day of imaging, worms were recovered for 1 hour on seeded RNAi plates without TMRE. For assays testing vitamin B1, OP50-seeded NGM plates were used either with or without 5 mg/mL vitamin B1. Worms were then put on slides with levamisole and were dissected for germline imaging. Images were captured on a Nikon eclipse Ti at 60x magnification, focusing on the most mature oocyte (-1 oocyte). All figures shown were from the same experiment, imaged under the same conditions. All images in each figure were processed in the same way across the entire image (e.g. adjusting for brightness and contrast).

Late-mated reproductive span assay

Late mated reproductive span assays were performed as previously described[51]. Briefly, hypochlorite-synchronized eggs were placed on plates seeded with OP50 *E. coli.* Starting on L4 stage, ~25 hermaphrodites were transferred to plates freshly seeded with HT115 *E. coli* containing either empty control vector, or RNAi plasmid. Worms were transferred to fresh RNAi plates every two days to avoid progeny accumulation. On the day of late mating, single hermaphrodites and three young *fog-2(q71)* males were transferred to plates seeded with the corresponding HT115 RNAi or control *E. coli* strain. Progeny production was assessed after 4-5 days. All late mating assays were performed at 20°C.

Full reproductive span

Reproductive span assays were performed either on plates as previously described [18], or using the lab-on-chip device *Ce*Lab[52]. For both reproductive span assay methods, hypochlorite-synchronized L4 hermaphrodites were mated for 24 h with young adult (day 1) *fog-2(q71)* males at a 1:3 ratio. For assays on plates, each hermaphrodite was moved daily to individual fresh plates until progeny production ceased for two consecutive days. The day of reproductive cessation was counted as the last day of viable progeny production preceding two consecutive days with no progeny. This was assessed by evaluating plates for progeny 2 days after the hermaphrodites had been moved to fresh plates. Successful mating was verified by evaluating the fraction of male progeny produced.

For *Ce*Lab reproductive span assays, chips were fabricated using standard soft lithography to create 200 parallel incubation arenas within each chip. Day 1 worms were loaded into the *Ce*Lab chip as previously described[52]. Animals were incubated in S-medium with 60 OD600 OP50-1, 50 mg/L streptomycin, and 10 mg/L nystatin. For RNAi experiments, bacteria were induced with 4 mM IPTG, pelleted, and resuspended with 2 ml S-medium with 50 mg/L streptomycin, 10 mg/L nystatin, 100 μg/mL carbenicillin and 4 mM IPTG before incubation. Worm survival was scored daily using *Ce*Aid[1]. After each scoring session, progeny were flushed out of the chip using M9 buffer solution for 20 minutes, and then the bacteria incubation solution was replenished. Animals were censored, if needed, on the day of loss. Matricide animals were censored the day after. All reproductive spans were performed at 20°C.

For experiments including supplements: all supplements were added to worms starting at day 1 of adulthood. Supplements were added at the appropriate concentration to 10x concentrated heat-killed OP50 *E. coli*. Bacteria were heat-killed by first pelleting and resuspending at 10X in double-distilled water. Bacteria were then heated at 65°C for 30 minutes before supplement addition.

Oocyte quality assay

Oocyte quality assays were performed as previously described [11,17]. For RNAi experiments, synchronized hermaphrodites were transferred to RNAi plates at L4 stage. Worms were transferred to fresh corresponding RNAi plates every two days to avoid progeny accumulation. Hermaphrodites were mated on day 3 of adulthood for 24 h with young adult (day 1) *fog-2(q71)* males at a 1:3 ratio. For all other

experiments, OP50-seeded NGM plates were used. For assays testing vitamin B1, OP50-seeded NGM plates were used with 5 mg/mL vitamin B1, starting at day 1 of adulthood. Hermaphrodites were mated at L4 stage for 24 h with young adult (day 1) *fog-2(q71)* males at a 1:3 ratio. Following mating, hermaphrodites were transferred to new plates. Mating was confirmed by the presence of male progeny. On the day of imaging, worms were mounted on slides with 2% agarose pads containing levamisole. Images were captured on a Nikon eclipse Ti at 60x magnification. Scoring was performed blindly, and each image was given a score based on the criteria detailed in the relevant figure.

Lifespan assay

Lifespan assays were performed either on plates as previously described[19], or using the lab-on-chip device *Ce*Lab[52]. For plates assays, synchronized hermaphrodites were placed on plates at day 1 of adulthood. Hermaphrodites were transferred to freshly seeded plates every other day when producing progeny, and 2-3 days thereafter.

For *Ce*Lab assays, chips were fabricated using standard soft lithography to create 200 parallel incubation arenas within each chip. Day 1 worms were loaded into *Ce*Lab. Animals were incubated in S-medium with 60 OD600 OP50-1, 50 mg/L streptomycin, and 10 mg/L nystatin.

For RNAi experiments, bacteria were induced with 4 mM IPTG, pelleted, and resuspended with bacteria with 2 ml S-medium with 50 mg/L streptomycin, 10 mg/L nystatin, 100 μg/mL carbenicillin and 4 mM IPTG before incubation. Survival was scored daily using *Ce*Aid[53]. After each scoring session, progeny were flushed out of the chip using M9 buffer solution for 20 minutes, and then the incubation solution was replenished. Worms were censored, if necessary, on the day of matricide, the appearance of abnormal vulva structures or loss. Animals were defined as dead when they no longer responded to touch. All lifespans were performed at 20°C.

For experiments including supplements: all supplements were added to worms starting at day 1 of adulthood. Supplements were added at the appropriate concentration to 10x concentrated heat-killed OP50 *E. coli*. Bacteria were heat-killed by first pelleting and resuspending at 10X in double-distilled water. Bacteria were then heated at 65°C for 30 minutes before supplement addition.

Germline mitochondria imaging

foxSi27 [Ppie-1::tomm-20::mKate2::HA::tbb-2 3' UTR (oxti385)] I; daf-2(e1370) III worms were synchronized and transferred to RNAi plates at the L4 stage. Hermaphrodites were then maintained on RNAi plates and were transferred to fresh corresponding RNAi plates every two days to avoid progeny accumulation.

On the day of germline imaging, worms were mounted on slides with 2% agarose pads and levamisole. Images were captured on either a Nikon eclipse Ti at 60x magnification or on a Nikon Ti-2 CSU-W1 spinning disk confocal with SoRa super-resolution technology. For Nikon Ti-2 CSU-W1 spinning disk confocal, a 100X/1.4 NA silicone oil objective was used for imaging, and a Hamamatsu BT Fusion sCMOS (6.5 μm pixel with 93% QE) camera was used for detection. Z stacks were acquired using 561 nm excitation wavelength to image mKate2-labeled mitochondria, and a single slice DIC image of the worm was acquired in the center of the Z stack for reference. Z stacks were processed using the Nikon NIS elements software. 3D volumetric views and movies were created using NIS Elements 'Volume projection' and movie maker, respectively.

Scoring was performed blindly. Each image was scored as normal (youthful oocyte characteristics: cuboidal shape, uniform size, organized in the gonad) or abnormal score while focusing on the mature oocytes. Images were processed in FIJI and Adobe Photoshop across the entire Z-stack. For each figure, images shown were from the same experiment, imaged on the same microscope at the same magnification, and with the same exposure. All images in each figure were processed in the same way across the entire image (e.g., max. intensity for Z-stack, adjusting for brightness and contrast).

Quantification and statistical analysis

For late-mated reproduction assays, Chi-square tests were used to compare the percentages of worm populations capable of progeny production. Full reproductive span and lifespan assays were assessed using standard Kaplan-Meier log-rank survival tests, with the first day of adulthood of synchronized hermaphrodites defined as t= 0. For oocyte quality experiments, chi-square tests were used to determine if there were significant differences between populations for each category of scored

oocyte phenotypes. Unpaired t-tests were used for BCAA levels comparisons, for normal/ abnormal germline mitochondria scoring, and for comparing mtROS. For BCAA assays, reads below the detection limit were excluded.

All experiments were repeated on separate days with separate, independent populations to confirm that results were reproducible. Additional statistical details of experiments, including sample size (with n representing the number of worms), can be found in the figure legends.

Software and algorithms

ImageJ2	[54]	
g:Profiler	[50]	https://biit.cs.ut.ee/gprofiler/gost
BioVenn	[55]	https://www.biovenn.nl/
BioRender		BioRender.com
GraphPad Prism 9, Version 9.4.1		GraphPad Software, San Diego, California USA, www.graphpad.com
UniProt	[56]	
Oasis	[57]	https://sbi.postech.ac.kr/oasis/

References

1. Duncan, F. E., Confino, R. & Pavone, M. E. Chapter 9 - Female Reproductive Aging: From Consequences to Mechanisms, Markers, and Treatments. in *Conn's Handbook of Models for Human Aging (Second Edition)* (eds. Ram, J. L. & Conn, P. M.) 109–130 (Academic Press, 2018). doi:https://doi.org/10.1016/B978-0-12-811353-0.00009-9.
2. Huber, S. & Fieder, M. Evidence for a maximum "shelf-life" of oocytes in mammals suggests that human menopause may be an implication of meiotic arrest. *Sci. Rep.* **8**, 14099 (2018).
3. Mathews, T. J. Mean Age of Mothers is on the Rise: United States, 2000–2014. 8 (2016).
4. Tilly, J. L. & Sinclair, D. A. Germline Energetics, Aging, and Female Infertility. *Cell Metab.* **17**, 838–850 (2013).
5. van der Reest, J., Nardini Cecchino, G., Haigis, M. C. & Kordowitzki, P. Mitochondria: Their relevance during oocyte ageing. *Ageing Res. Rev.* **70**, 101378 (2021).
6. Andux, S. & Ellis, R. E. Apoptosis maintains oocyte quality in aging Caenorhabditis elegans females. *PLoS Genet.* **4**, e1000295 (2008).
7. Ovarian Aging: Mechanisms and Clinical Consequences | Endocrine Reviews | Oxford Academic. https://academic.oup.com/edrv/article/30/5/465/2355057?login=false.
8. te Velde, E. R. & Pearson, P. L. The variability of female reproductive ageing. *Hum. Reprod. Update* **8**, 141–154 (2002).
9. Hughes, S. E., Evason, K., Xiong, C. & Kornfeld, K. Genetic and pharmacological factors that influence reproductive aging in nematodes. *PLoS Genet.* **3**, e25 (2007).
10. Luo, S., Kleemann, G. A., Ashraf, J. M., Shaw, W. M. & Murphy, C. T. TGF-β and Insulin Signaling Regulate Reproductive Aging via Oocyte and Germline Quality Maintenance. *Cell* **143**, 299–312 (2010).
11. Templeman, N. M. *et al.* Insulin Signaling Regulates Oocyte Quality Maintenance with Age via Cathepsin B Activity. *Curr. Biol. CB* **28**, 753-760.e4 (2018).
12. Huang, C., Xiong, C. & Kornfeld, K. Measurements of age-related changes of physiological processes that predict lifespan of Caenorhabditis elegans. *Proc. Natl. Acad. Sci. U. S. A.* **101**, 8084–8089 (2004).
13. Athar, F. & Templeman, N. M. C. elegans as a model organism to study female reproductive health. *Comp. Biochem. Physiol. A. Mol. Integr. Physiol.* **266**, 111152 (2022).
14. Llonch, S. *et al.* Single human oocyte transcriptome analysis reveals distinct maturation stage-dependent pathways impacted by age. *Aging Cell* **20**, e13360 (2021).
15. Zhang, D., Keilty, D., Zhang, Z. & Chian, R. Mitochondria in oocyte aging: current understanding. *Facts Views Vis. ObGyn* **9**, 29–38 (2017).
16. Rodríguez-Nuevo, A. *et al.* Oocytes maintain ROS-free mitochondrial metabolism by suppressing complex I. *Nature* **607**, 756–761 (2022).
17. Luo, S., Kleemann, G. A., Ashraf, J. M., Shaw, W. M. & Murphy, C. T. TGF-β and insulin signaling regulate reproductive aging via oocyte and germline quality maintenance. *Cell* **143**, 299–312 (2010).
18. Luo, S., Shaw, W. M., Ashraf, J. & Murphy, C. T. TGF-beta Sma/Mab signaling mutations uncouple reproductive aging from somatic aging. *PLoS Genet.* **5**, e1000789 (2009).
19. Kenyon, C., Chang, J., Gensch, E., Rudner, A. & Tabtiang, R. A C. elegans mutant that lives twice as

long as wild type. *Nature* **366**, 461–464 (1993).
20. Bratic, I. *et al.* Mitochondrial DNA level, but not active replicase, is essential for Caenorhabditis elegans development. *Nucleic Acids Res.* **37**, 1817–1828 (2009).
21. Gitschlag, B. L. *et al.* Homeostatic responses regulate selfish mitochondrial genome dynamics in C. elegans. *Cell Metab.* **24**, 91–103 (2016).
22. Tsang, W. Y. & Lemire, B. D. Mitochondrial Genome Content Is Regulated during Nematode Development. *Biochem. Biophys. Res. Commun.* **291**, 8–16 (2002).
23. Murphy, C. T. *et al.* Genes that act downstream of DAF-16 to influence the lifespan of Caenorhabditis elegans. *Nature* **424**, 277–283 (2003).
24. Valerio, A., D'Antona, G. & Nisoli, E. Branched-chain amino acids, mitochondrial biogenesis, and healthspan: an evolutionary perspective. *Aging* **3**, 464–478 (2011).
25. Agarwal, S. & Ganesh, S. Perinuclear mitochondrial clustering, increased ROS levels, and HIF1 are required for the activation of HSF1 by heat stress. *J. Cell Sci.* jcs.245589 (2020) doi:10.1242/jcs.245589.
26. Mansfeld, J. *et al.* Branched-chain amino acid catabolism is a conserved regulator of physiological ageing. *Nat. Commun.* **6**, 10043 (2015).
27. Branched Chain Amino Acid Assay Kit / BCAA Assay Kit (ab83374) | Abcam. https://www.abcam.com/branched-chain-amino-acid-assay-kit--bcaa-assay-kit-ab83374.html.
28. Blair, P. V. *et al.* Dietary Thiamin Level Influences Levels of Its Diphosphate Form and Thiamin-Dependent Enzymic Activities of Rat Liver. *J. Nutr.* **129**, 641–648 (1999).
29. Skvorak, K. J. Animal models of maple syrup urine disease. *J. Inherit. Metab. Dis.* **32**, 229–246 (2009).
30. Mann, G., Mora, S., Madu, G. & Adegoke, O. A. J. Branched-chain Amino Acids: Catabolism in Skeletal Muscle and Implications for Muscle and Whole-body Metabolism. *Front. Physiol.* **12**, (2021).
31. Palmieri, F., Monné, M., Fiermonte, G. & Palmieri, L. Mitochondrial transport and metabolism of the vitamin B-derived cofactors thiamine pyrophosphate, coenzyme A, FAD and NAD+, and related diseases: A review. *IUBMB Life* **n/a**,.
32. Harris, R. A. *et al.* MOLECULAR BASIS FOR MAPLE SYRUP URINE DISEASE. 21.
33. Marrs, C. & Lonsdale, D. Hiding in Plain Sight: Modern Thiamine Deficiency. *Cells* **10**, 2595 (2021).
34. Martel, J. L., Kerndt, C. C., Doshi, H. & Franklin, D. S. Vitamin B1 (Thiamine). in *StatPearls* (StatPearls Publishing, 2022).
35. Smith, T. J. *et al.* Thiamine deficiency disorders: a clinical perspective. *Ann. N. Y. Acad. Sci.* **1498**, 9–28 (2021).
36. Office of Dietary Supplements - Thiamin. https://ods.od.nih.gov/factsheets/Thiamin-HealthProfessional/.
37. Institute of Medicine (US) Standing Committee on the Scientific Evaluation of Dietary Reference Intakes and its Panel on Folate, Other B Vitamins, and Choline. *Dietary Reference Intakes for Thiamin, Riboflavin, Niacin, Vitamin B6, Folate, Vitamin B12, Pantothenic Acid, Biotin, and Choline*. (National Academies Press (US), 1998).
38. Brenner, S. The genetics of Caenorhabditis elegans. *Genetics* **77**, 71–94 (1974).
39. Ahier, A. *et al.* Affinity purification of cell-specific mitochondria from whole animals resolves patterns of genetic mosaicism. *Nat. Cell Biol.* **20**, 1–9 (2018).
40. Daniele, J. R., Heydari, K., Arriaga, E. A. & Dillin, A. Identification and Characterization of Mitochondrial Subtypes in Caenorhabditis elegans via Analysis of Individual Mitochondria by Flow Cytometry. *Anal. Chem.* **88**, 6309–16 (2016).
41. Gandre, S. & van der Bliek, A. M. Mitochondrial division in Caenorhabditis elegans. *Methods Mol. Biol. Clifton NJ* **372**, 485–501 (2007).
42. Lesnik, C. & Arava, Y. Isolation of mRNAs Associated with Yeast Mitochondria to Study Mechanisms of Localized Translation. *J. Vis. Exp. JoVE* (2014) doi:10.3791/51265.
43. Wieckowski, M. R., Giorgi, C., Lebiedzinska, M., Duszynski, J. & Pinton, P. Isolation of mitochondria-associated membranes and mitochondria from animal tissues and cells. *Nat. Protoc.* **4**, 1582–1590 (2009).
44. Ma, J. H. *et al.* Comparative proteomic analysis of the mitochondria-associated ER membrane (MAM) in a long-term type 2 diabetic rodent model. *Sci. Rep.* **7**, 1–17 (2017).
45. Annunziata, I., Patterson, A. & d'Azzo, A. Mitochondria-associated ER membranes (MAMs) and glycosphingolipid enriched microdomains (GEMs): isolation from mouse brain. *J. Vis. Exp. JoVE* (2013) doi:10.3791/50215.
46. S-Trap™. https://www.protifi.com/s-trap/.
47. Cox, J. & Mann, M. MaxQuant enables high peptide identification rates, individualized p.p.b.-range mass accuracies and proteome-wide protein quantification. *Nat. Biotechnol.* **26**, 1367–

1372 (2008).
48. Cox, J. *et al.* Accurate Proteome-wide Label-free Quantification by Delayed Normalization and Maximal Peptide Ratio Extraction, Termed MaxLFQ *. *Mol. Cell. Proteomics* **13**, 2513–2526 (2014).
49. Tyanova, S. *et al.* The Perseus computational platform for comprehensive analysis of (prote)omics data. *Nat. Methods* **13**, 731–740 (2016).
50. Raudvere, U. *et al.* g:Profiler: a web server for functional enrichment analysis and conversions of gene lists (2019 update). *Nucleic Acids Res.* **47**, W191–W198 (2019).
51. Templeman, N. M., Cota, V., Keyes, W., Kaletsky, R. & Murphy, C. T. CREB Non-autonomously Controls Reproductive Aging through Hedgehog/Patched Signaling. *Dev. Cell* **54**, 92-105.e5 (2020).
52. Sohrabi, S., Cota, V. & Murphy, C. T. CeLab, a Microfluidic Platform for the Study of Life History Traits, reveals Metformin and SGK-1 regulation of Longevity and Reproductive Span. 2023.01.09.523184 Preprint at https://doi.org/10.1101/2023.01.09.523184 (2023).
53. Sohrabi, S., Moore, R. S. & Murphy, C. T. CeAid: a smartphone application for logging and plotting Caenorhabditis elegans assays. *G3 GenesGenomesGenetics* **11**, jkab259 (2021).
54. Abramoff, M. D., Magalhães, P. J. & Ram, S. J. Image processing with ImageJ. *Biophotonics Int.* **11**, 36–42 (2004).
55. Hulsen, T., de Vlieg, J. & Alkema, W. BioVenn - a web application for the comparison and visualization of biological lists using area-proportional Venn diagrams. *BMC Genomics* **9**, 488 (2008).
56. UniProt: the Universal Protein Knowledgebase in 2023 | Nucleic Acids Research | Oxford Academic. https://academic.oup.com/nar/article/51/D1/D523/6835362?login=false.
57. OASIS: Online Application for the Survival Analysis of Lifespan Assays Performed in Aging Research | PLOS ONE. https://journals-plos-org.ezproxy.princeton.edu/plosone/article?id=10.1371/journal.pone.0023525.

Supplementary Tables and Figures

Supplementary Table 1: Proteomic data
LFQ intensity of all peptides detected by LC-MS/MS proteomic analysis in mitochondria fractions isolated from young (day 1 adult) and reproductively aged (day 5 adult) wild-type worms and from *daf-2(e1370)* mutants. The table shows the significant proteins (i.e., proteins with more than one peptide, fold change>2, and q-value< 0.05) for each comparison between the different conditions.

Supplementary Table 2: Reproductive span data
Statistical data for reproductive spans assays.

Supplementary Table 3: Lifespan data
Statistical data for lifespans assays.

Supplementary Table 4: Late-mated reproduction data.
Statistical data for late-mated reproduction assays.

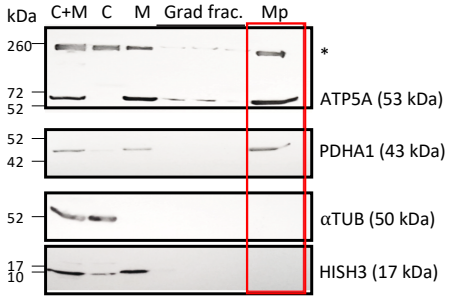

Supplementary Figure 1: Highly purified mitochondria are isolated from *C. elegans*
Representative western blot of the different cellular fractions. Mitochondrial protein markers (ATP5A and PDHA1) are prominently enriched in the highly purified mitochondria fraction, while other cellular protein markers (αTUB and HISH3) are enriched in the cytosol and nuclei fractions, respectively.C+M- total homogenate (cytosolic and membranal cellular fractions), C- cytosolic fraction, M- crude membranes fraction, Grad frac- fractions of the gradient (other than the highly purified mitochondria), Mp- highly purified mitochondria. PDHA1- pyruvate dehydrogenase complex, αTUB- alpha tubulin, HISH3- histone H3. Asterisk represents a non-specific band detected when using the anti-ATP5A antibody.

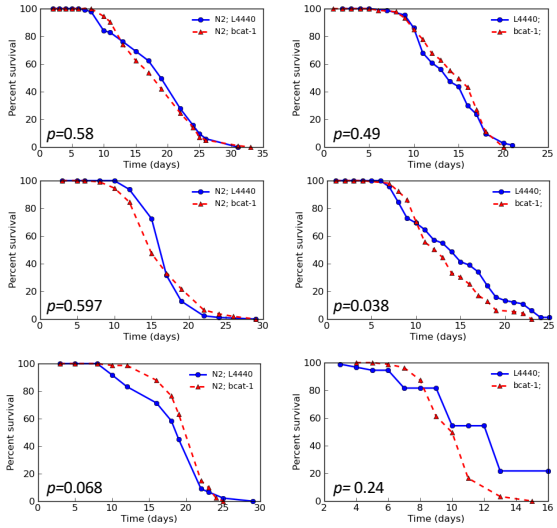

Supplementary Figure 2: Downregulating *bcat-1* in wild-type worms does not affect lifespan
Adult-only knockdown of *bcat-1* does not affect the lifespan of wild-type animals. Lifespan data of 6 biological replicates are shown. Results are plotted as Kaplan-Meier survival curves, and the *p*-value was calculated using Mantel-Cox log-ranking. Statistical data is detailed in Table S3.